Ribosome-inactivating protein and apoptosis: abrin causes cell death via mitochondrial pathway in Jurkat cells

Sriram NARAYANAN*, Avadhesha SUROLIA* and Anjali A. KARANDE†[1]

*Molecular Biophysics Unit, Indian Institute of Science, Bangalore 560012, India, and †Department of Biochemistry, Indian Institute of Science, Bangalore 560012, India

Abrin belongs to the type II family of ribosome-inactivating proteins comprising a galactose-binding B chain coupled with a toxic A chain through a single disulphide linkage. Apart from its RNA-*N*-glycosidase activity, another role that has been recently ascribed to abrin was the induction of apoptosis. Studies were undertaken to determine the kinetics of these two activities. In the present study, we report that the signal for apoptosis is triggered at a time point later than the inhibition of protein synthesis. This apoptotic pathway induced by abrin is caspase 3-dependent but caspase 8-independent and involves mitochondrial membrane potential damage and reactive oxygen species production. Overexpression of B-cell lymphocytic-leukaemia proto-oncogene 2 was found to block this apoptotic pathway.

Key words: abrin, apoptosis, DNA fragmentation, mitochondrial membrane potential, protein synthesis inhibition, reactive oxygen species.

INTRODUCTION

RIP (ribosome-inactivating protein) toxins are of two types: type I RIPs, which are single-subunit proteins, e.g. saporin, gelonin and momordin, and type II RIPs, which are heterodimeric and made up of A and B subunits linked by a single disulphide bond, e.g. ricin, abrin and mistletoe lectin (ML) [1–3]. Type I RIPs and the A subunit of type II RIPs are RNA-N-glycosidases, which catalyse the cleavage of the adenine residue A4324 from the 28 S rRNA, thereby inhibiting protein synthesis, as determined in cell-free systems [4,5]. It was also shown that some of the RIPs are capable of depurinating rRNA at more than one site [6], indicating their broad specificity. Type II RIPs bind to cell-surface receptors containing terminal galactose, through their B subunit, enter inside the cell by receptor-mediated endocytosis [7] and are transported to endoplasmic reticulum (ER) by retrograde pathway [8]. The intersubunit disulphide bond, which is essential for their toxicity [9], is reduced in the ER followed by translocation of the A-chain to cytosol by an ER-associated degradation pathway [10,11]. Besides inhibition of protein synthesis, RIPs have been shown to induce apoptosis or programmed cell death (PCD) [12–14]. Vervecken et al. [15] have demonstrated that ML I holotoxin alone induced apoptosis in MOLT-4, a human T-cell line, and human peripheral blood lymphocytes, whereas isolated A or B chains did not. Also, it has been reported that cell death induced by the RIPs, such as ricin, modeccin, diphtheria toxin (DT) and pseudomonas toxin, involves caspase-like and serine proteases [16]. In addition, it was reported that during ricin-induced ribosomal inactivation, the cellular ATP and NAD^+ levels were depleted before cell death [17]. The inactivation of antioxidant protein has recently been proposed to play a role in the abrin-induced cell-death pathway [18]. Although the apoptotic pathways induced by classical apoptosis inducers like tumour necrosis factor-α, FasL (Fas ligand) and other small molecules such as etoposide, staurosporine, etc. are well studied, a lacuna exists in the knowledge of cell-death pathways induced by plant toxins that bring about inhibition of protein synthesis. The studies reported here attempt to bridge this gap.

MATERIALS AND METHODS

Materials

Sepharose 6B, Sephadex G100, RPMI-1640, BSA, AcOr (Acridine Orange), EtBr (ethidium bromide), FBS (foetal bovine serum), PI (propidium iodide), RNase A, proteinase K, DCFH-DA (2′,7′-dichlorodihydrofluorescein diacetate), and pancaspase inhibitor, Z-VAD-FMK [*N*-benzyloxycarbonyl-Val-Ala-Asp (O-Me)-fluoromethyl ketone], were purchased from Sigma (St. Louis, MO, U.S.A.). [^{3}H]Leucine was obtained from BRIT, India. Ac-DEVD-AMC (*N*-acetyl-Asp-Glu-Val-Asp-7-amino-4-methylcoumarin) and Ac-DEVD-CHO [*N*-acetyl-Asp-Glu-Val-Asp-CHO (aldehyde)] were procured from Becton Dickinson (Franklin Lakes, NJ, U.S.A.). JC-1 (5,5′,6,6′-tetrachloro-1,1′,3,3′-tetraethylbenzimidazolyl carbocyanine iodide) was purchased from Molecular Probes (Eugene, OR, U.S.A.). Rabbit anticaspase 3 antibody and phototope-HRP (where HRP stands for horseradish peroxidase) Western-blot detection system were from Cell Signaling Technology (Beverly, MA, U.S.A.). The cell-permeable caspase 3 inhibitor peptide I was from Calbiochem. All other reagents were of analytical grade.

Cell culture

JR4, J16 Bcl-2 (where Bcl-2 stands for B-cell lymphocytic-leukaemia proto-oncogene 2) and A3 I9.2 clones of Jurkat cells and MOLT-4 cells (human T-cell lines) were cultured in RPMI 1640, supplemented with 10 % (v/v) FBS, 100 i.u./ml penicillin

Abbreviations used: Ac-DEVD-AMC, *N*-acetyl-Asp-Glu-Val-Asp-7-amino-4-methylcoumarin; Ac-DEVD-CHO, *N*-acetyl-Asp-Glu-Val-Asp-CHO (aldehyde); AcOr, Acridine Orange; Bcl-2, B-cell lymphocytic-leukaemia proto-oncogene 2; DCFH-DA, 2′,7′-dichloro dihydro fluorescein diacetate; EtBr, ethidium bromide; FasL, Fas ligand; FBS, foetal bovine serum; JC-1, 5,5′,6,6′-tetrachloro-1,1′,3,3′-tetraethylbenzimidazolyl carbocyanine iodide; ML, mistletoe lectin; MMP, mitochondrial membrane potential; PARP, poly(ADP-ribose) polymerase; PI, propidium iodide; RIP, ribosome-inactivating protein; ROS, reactive oxygen species.

[1] To whom correspondence should be addressed (e-mail anjali@biochem.iisc.ernet.in).

and 100 i.u./ml streptomycin in a humidified air/CO_2 (19:1) atmosphere. The J16 Bcl-2, a Jurkat clone that overexpresses the anti-apoptotic protein Bcl-2, is a gift from Prof. Schulze-Osthoff (Institute of Molecular Medicine, University of Duesseldorf, Germany).

Purification of abrin

The protein was purified from the matured seeds of *Abrus precatorius* as described previously [19]. Briefly, the seed kernels were soaked overnight in 5 % (v/v) acetic acid and homogenized. The crude extract was subjected to 30 % (w/v) ammonium sulphate precipitation and the supernatant subsequently subjected to 90 % (w/v) ammonium sulphate precipitation, followed by extensive dialysis against 10 mM phosphate buffer, containing 150 mM NaCl, pH 7.4 (PBS). The dialysate was centrifuged at 14 000 ***g*** at 4 °C for 15 min and the supernatant was loaded on to lactamyl-Sepharose affinity column [20,21] pre-equilibrated with 10 mM PBS. The unbound proteins were removed by washing with PBS. The bound proteins were eluted with 0.4 M lactose. The fractions containing abrin were pooled and loaded on to Sephadex G100 gel-filtration column equilibrated with 20 mM PBS. The fractions corresponding to $M_w \sim 60$ kDa were pooled, dialysed extensively and freeze-dried. Protein concentration was determined based on molar absorption coefficient ε of 100 170 $M^{-1} \cdot cm^{-1}$ [19].

Protein synthesis inhibition assay

The assay was carried out as described in [22]. Jurkat cells (1×10^6 cells/ml) were cultured in the absence or in the presence of different concentrations of abrin in 200 μl of leucine-free RPMI 1640 medium. After the addition of abrin, 20 μCi of [^{3}H]leucine was added at various time intervals, and the cells were incubated at 37 °C for 30 min. After the addition of 100 μg of BSA as carrier protein, the total protein was precipitated with 20 % (w/v) trichloroacetic acid and the mixture was centrifuged at 20 000 ***g*** for 10 min at 4 °C. The precipitate was then washed with 10 % trichloroacetic acid, solubilized in 20 μl of 2 M NaOH, and the radioactivity was measured in a scintillation counter (Wallac, Finland).

AcOr–EtBr staining

Briefly, Jurkat cells were cultured in the presence or absence of different concentrations of abrin for different time intervals. At each time interval, the cells were centrifuged at 300 ***g*** for 5 min and resuspended in 25 μl of medium along with 1 μl of dye mixture of AcOr and EtBr (100 μg/ml each in PBS) [23]. The cells were observed under a fluorescence microscope (Carl Zeiss, Gottingen, Germany) using a blue filter to score for apoptosis and secondary necrosis based on their fluorescence and nuclear morphology.

PI staining and FACScan analysis for apoptosis

As described elsewhere [24], Jurkat cells (1×10^6 cells/ml) were treated with 10 ng/ml (0.16 nM) of abrin in RPMI 1640 medium supplemented with 10 % (v/v) FBS for various time intervals. At the end of each time period, the cells were centrifuged at 300 ***g*** for 5 min, resuspended in 100 μl of 50 mM PBS and fixed with ice-cold 70 % (v/v) ethanol for 30 min at -20 °C. The cells were pelleted and washed once with PBS and stained with PI (50 μg/ml) staining solution containing 100 μg/ml RNase A, 1 % (v/v) Triton X-100 and 40 mM sodium citrate for 60 min at 37 °C. The cells were then analysed by a fluorescence-activated flow cytometer (FACScan; Becton Dickinson). A similar assay was performed using the caspase 8 mutant Jurkat cell line, A3 I9.2, to determine the role of caspase 8 in abrin-induced apoptotic pathway and with J16 Bcl-2 cells to study the effect of Bcl-2 overexpression on abrin-induced cell death.

DNA fragmentation assay

DNA fragmentation assay was performed as described earlier [25]. Jurkat and MOLT-4 cells (1×10^6/ml) cultured in the presence of abrin (0.16 nM) for various time intervals were centrifuged at 300 ***g*** at room temperature (25 °C) for 5 min, suspended in 100 μl of 50 mM PBS and fixed with ice-cold 70 % (v/v) ethanol for 30 min. The cells were centrifuged again at 800 ***g*** for 5 min at 4 °C. After removing ethanol completely, the cells were resuspended in 0.1 M citrate buffer (pH 7.8) and incubated at room temperature for 30 min with occasional mixing. The cells were then centrifuged at 1000 ***g*** for 5 min at 4 °C and the supernatant was concentrated. NP40 (Nonidet P40; 10 μl, 0.25 %, v/v) and RNase A (3 μg) were added to the concentrated solution and incubated at 50 °C for 30 min. Then 3 μg of proteinase K was added and the incubation was continued for 30 min at 37 °C. DNA-loading buffer [10 μl; 0.25 % (w/v) Bromophenol Blue, 0.25 % (w/v) xylene cyanol in 30 % (v/v) glycerol in water] was added to the mixture and loaded on to a 1 % (w/v) agarose gel and electrophoresed at 2 V/cm for 16 h. The gel was then stained with ethidium bromide (5 μg/ml) for 15 min, destained in water for 5 min and observed under UV transilluminator.

Caspase 3 assay

The assay was performed by monitoring cleavage of the caspase 3-specific fluorogenic substrate (Becton Dickinson) according to the manufacturer's instructions. Jurkat cells (1×10^6 ml^{-1}) were cultured in the absence or presence of abrin (0.16 nM) for various time intervals. At the end of each time interval, the cells were washed once with PBS and stored at -20 °C. Later the cells were suspended in lysis buffer [10 mM Tris/HCl, pH 7.5/10 mM NaH_2PO_4/Na_2HPO_4, pH 7.5/130 mM NaCl/1 % (v/v) Triton X-100]. Lysate (100 μl) was added to 1 ml of reaction buffer (1.4 M NaCl/27 mM KCl/100 mM KH_2PO_4/K_2HPO_4, pH 7.5), containing 100 ng of the fluorogenic substrate Ac-DEVD-AMC and incubated at 37 °C for 1 h. Fluorescence was measured with excitation at 380 nm and emission at 420 nm. For establishing the specificity of the reaction, the caspase 3 inhibitor, Ac-DEVD-CHO was used.

Western-blot analysis of caspase 3 cleavage

JR4 Jurkat cells (2×10^6/ml) were cultured with abrin for various time periods and were lysed in hypotonic lysis buffer (10 mM phosphate buffer, pH 7.4). An equal amount of total protein was electrophoresed on SDS/polyacrylamide (12.5 % gel) and transferred on to a nitrocellulose membrane. The cleavage of caspase 3 was demonstrated using an antibody raised against caspase 3, and the blot was developed using enhanced chemiluminescence.

Measurement of loss of MMP (mitochondrial membrane potential)

The change in MMP ($\triangle\Psi_m$) was measured using the potentiometric dye JC-1 as described elsewhere [26]. Briefly, Jurkat cells

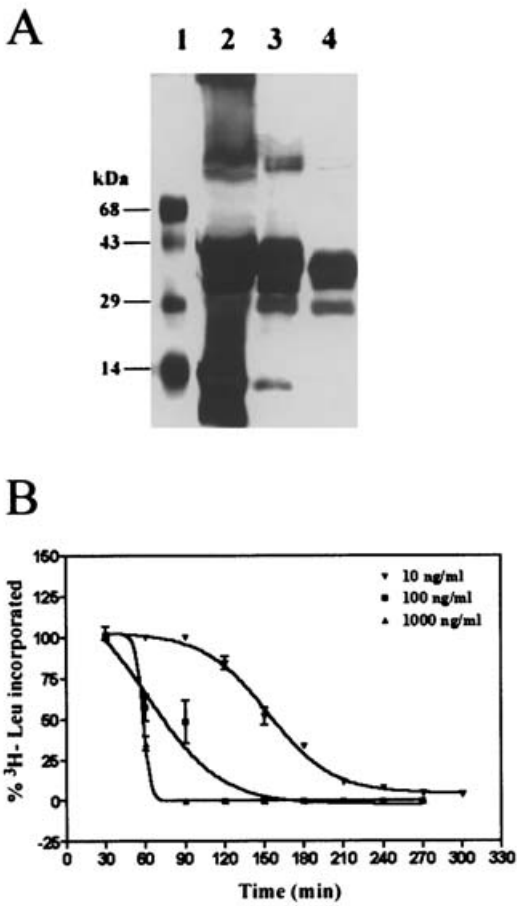

Figure 1 Inhibition of protein synthesis in Jurkat cells

(**A**) Purification of abrin: abrin was purified as described in the text and the protein samples from various steps of purification were electrophoresed under reducing conditions on a 12.5 % polyacrylamide gel and stained by silver. Lane 1, molecular-mass markers; lane 2, 90 % ammonium sulphate precipitation of *Abrus precatorius* homogenate; lane 3, lactamyl-Sepharose affinity column lactose eluate; and lane 4, abrin obtained by gel filtration. (**B**) Kinetics of protein synthesis inhibition: cells were cultured with or without abrin, and protein synthesis was monitored by [^{3}H]leucine incorporation for 30 min as described in the text. Inhibition of protein synthesis was expressed as percentage of radioactivity incorporated into test samples compared with untreated control cells.

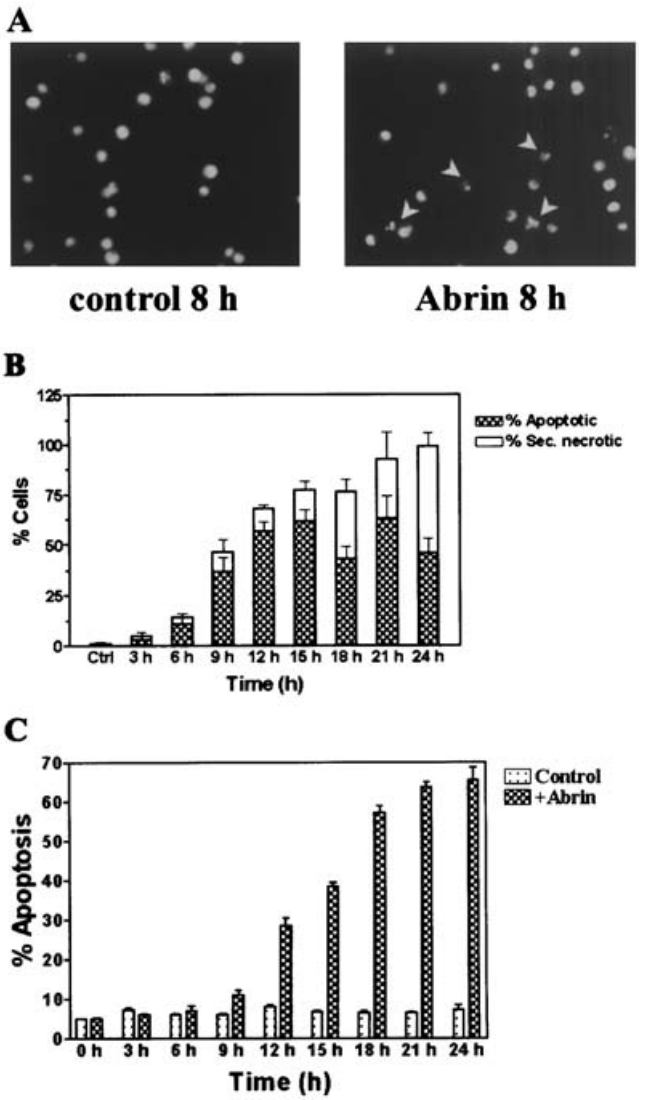

Figure 2 Abrin-induced apoptosis in Jurkat cells

(**A**) AcOr–EtBr staining: JR4 Jurkat cells were cultured in the presence or absence of 0.16 nM abrin for 8 h, followed by staining with AcOr–EtBr and viewed under a fluorescence microscope using a blue filter. The arrowheads indicate cells undergoing apoptosis. (**B**) Abrin-induced apoptosis proceeds to secondary necrosis: JR4 Jurkat cells treated with abrin were stained with AcOr–EtBr and the cells showing apoptotic and secondary necrotic morphologies were counted. (**C**) DNA fragmentation induced by abrin as determined by PI staining and flow cytometry: Jurkat cells were cultured in the presence of 0.16 nM abrin for the indicated time intervals, after which the cells were fixed, stained with PI and analysed by flow cytometry. PBS-treated cells served as negative control ('control' in Figure). The percentage of cells in sub-G1 peak was quantified and plotted against time.

(JR4 and J16 Bcl-2) were treated with abrin (0.16 nM) for the indicated time periods. At the end of treatments, the cells were stained with 2.5 μg/ml of JC-1 dye and incubated at 37 °C for 15 min. The cells were then washed once with ice-cold FACS buffer [PBS containing 2 % (v/v) FBS], resuspended in the same and analysed immediately by flow cytometry for red and green fluorescence (FACScan; Becton Dickinson).

ROS (reactive oxygen species) assay

The involvement of ROS in abrin-induced apoptotic pathway was studied using the dye 2′,7′-dichloro dihydro fluorescein diacetate (DCFH-DA) [27]. Briefly, Jurkat cells were first pretreated with DCFH-DA (20 μM) for 30 min and then treated with abrin (0.16 nM) for the indicateds time periods. At the end of treatments, the cells were washed once with ice-cold FACS buffer, resuspended in the same and analysed immediately by flow cytometry for green fluorescence at 530 nm.

RESULTS

Purification of abrin

Abrin was purified from matured seeds of *Abrus precatorius* in three steps. The SDS/PAGE profile of abrin and samples from different steps of purification are shown in Figure 1(A). As reported in [19], it was observed that the A chain was 30 kDa, whereas the B chain was 33 kDa. As there are two isoforms of abrin (I and III) that have the same A chain, but different B chains [28], two closely running bands are observed on the 12.5 % gel corresponding to 33 kDa (Figure 1A). However, as reported by

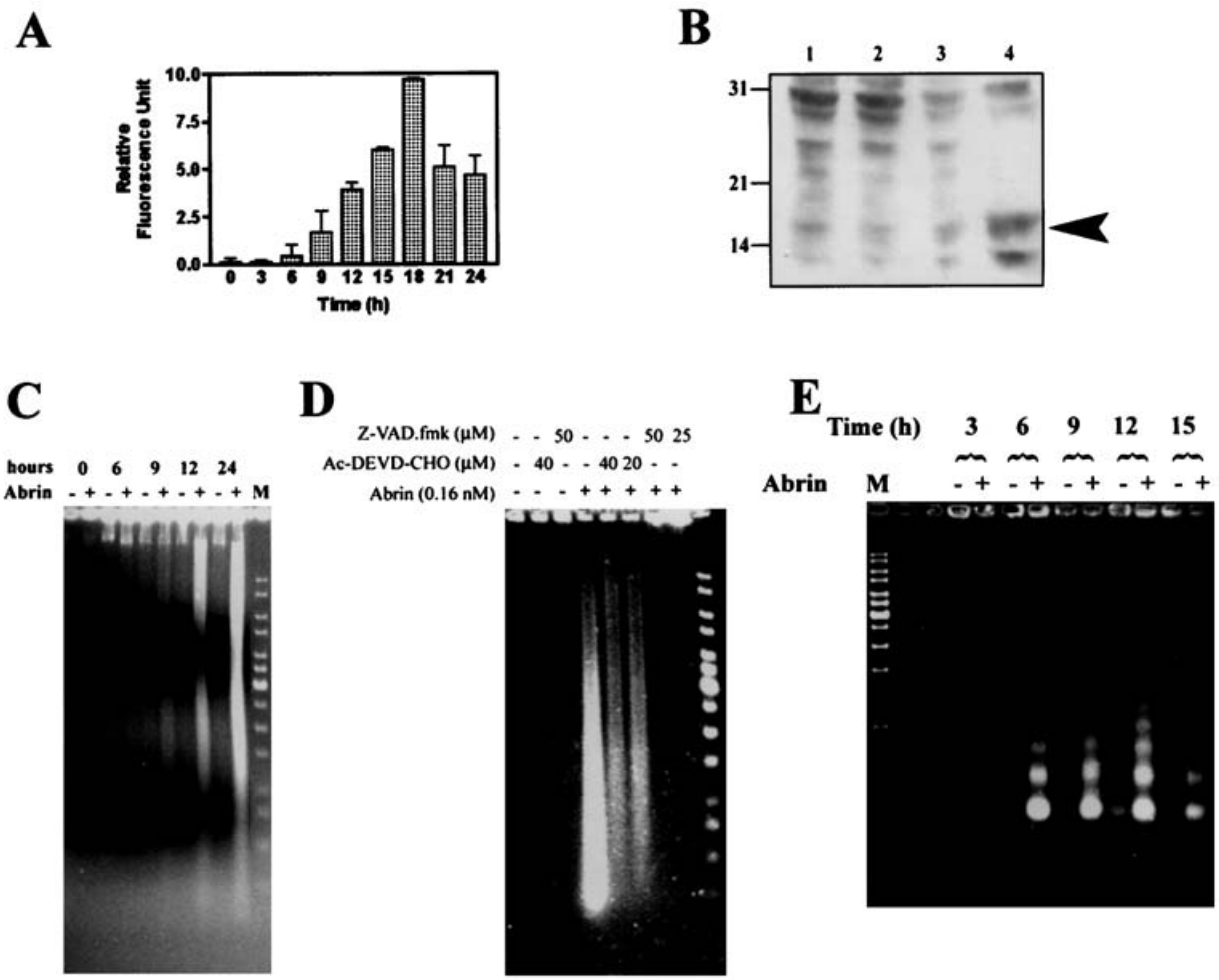

Figure 3 Activation of caspase 3 and DNA fragmentation by abrin

(**A**) Caspase 3 activation by abrin: Jurkat cells were cultured in the presence of 0.16 nM abrin for the time intervals indicated and assayed for caspase 3 activity with caspase 3-specific substrate Ac-DEVD-AMC and analysed using a fluorimeter by excitation at 380 nm and emission at 440 nm. All the readings were normalized for control readings for each time interval obtained in the presence of caspase 3 inhibitor Ac-DEVD-CHO. (**B**) Caspase 3 Western blot: JR4 Jurkat cells were treated with abrin for the indicated time periods and were lysed on ice in 10 mM phosphate buffer (pH 7.4) for 30 min. An equal amount (120 μg) of total protein was loaded on to each lane of SDS/polyacrylamide (12.5 % gel). The separated proteins were transferred on to a nitrocellulose membrane and probed with anti-caspase 3 antibody. Lane 1, untreated control cell lysate; lanes 2–4, lysates of cells treated with abrin for 3, 12 and 15 h respectively. The cleaved form of caspase 3 is indicated by an arrowhead. Molecular mass (kDa) is indicated on the left-hand side. (**C**) DNA fragmentation by agarose gel electrophoresis: Jurkat cells were cultured in the presence of 0.16 nM abrin for the time periods indicated. The cells were processed as described in the text and the fragmented DNA was electrophoresed on a 1 % agarose gel, stained with EtBr and viewed under UV light. (**D**) Caspase 3 inhibition abrogates abrin-induced DNA fragmentation: Jurkat cells preincubated with cell-permeable caspase 3 inhibitor peptide I, or with cell-permeable-pan-caspase inhibitor Z-VAD-FMK were cultured in the presence of 0.16 nM abrin and processed as mentioned above. The last lane was loaded with 1 kb DNA ladder as marker. (**E**) DNA laddering in MOLT-4 cells treated with abrin: MOLT-4 cells were treated with abrin (0.16 nM) and were processed as described in the Materials and methods section for visualizing the apoptotic DNA fragmentation on agarose gel.

Hegde et al. [29], there is no difference between the isoforms with respect to either toxicity or binding. Hence, the total abrin preparation as such was used for further studies.

Kinetics of protein synthesis inhibition

The amount of protein synthesized was determined by incorporation of [^{3}H]leucine in the total protein precipitate. The inhibitory activity of abrin in protein synthesis is expressed as percentage of [^{3}H]leucine incorporated into the treated cells when compared with untreated cells. As can be seen from Figure 1(B), the lag period in the inhibition curves decreased markedly with increase in toxin concentration. The lag phase was 90 min for the lowest concentration (0.16 nM), and the protein synthesis was inhibited completely by 4 h.

Abrin induces apoptosis in Jurkat cells

To determine whether the abrin-treated cells die of apoptosis or necrosis, AcOr–EtBr staining was performed. Jurkat cells cultured with different concentrations of abrin for different time intervals showed a dose-dependent decrease in the time required for DNA condensation and nuclear fragmentation, the hallmark of cells undergoing apoptosis. It took just 4 h for concentrations up to 50 ng/ml to induce changes in nuclear morphology (results not shown), whereas it took 8 h to observe the same with 10 ng/ml (Figure 2A). However, concentrations below 10 ng/ml did not show any apoptosis up to 12 h (results not shown). Hence, the concentration 10 ng/ml (0.16 nM) was chosen for all further apoptosis assays. After 15 h of abrin treatment, the cells were observed to enter secondary necrosis in late apoptosis, when the membrane integrity is lost (Figure 2B).

Kinetics of apoptosis induction

The kinetics of apoptosis induced by abrin was studied by PI staining and DNA fragmentation. Jurkat cells were cultured with 10 ng/ml abrin for different time intervals up to 24 h. Apoptosis was observed only after 6 h, and then there was a time-dependent increase in the percentage of apoptotic cell population, reaching a maximum of 70 % by 21 h as determined by FACScan analysis after PI staining (Figure 2C).

Jurkat cells were treated with 10 ng/ml of abrin for different time intervals up to a maximum of 24 h and analysed. DNA fragmentation was first seen at 9 h and it increased with time (Figure 3C). As a typical DNA ladder pattern was not seen in the case of Jurkat cells, the experiment was repeated on another human T-cell line, MOLT-4. As is evident from Figure 3(E), abrin treatment of MOLT-4 cells resulted in DNA ladder formation.

Caspase 3 is one of the effector caspases known to degrade many structural and regulatory proteins as well as proteins involved in DNA repair [30,31]. It is also known to trigger DNA fragmentation during apoptosis [32]. We studied the role of caspase 3 in abrin-induced apoptosis and the kinetics of its activation. The activity of caspase 3 was determined by fluorescence emission of the cleaved substrate Ac-DEVD-AMC. As shown in Figure 3(A), a time-dependent increase in fluorescence was seen, starting at 9 h. When Jurkat cells were cultured with abrin in the presence of the cell-permeable caspase 3 inhibitor peptide or with the pan-caspase inhibitor, Z-VAD-FMK, reduction in DNA fragmentation was observed (Figure 3D) confirming that the DNA fragmentation induced by abrin indeed occurs via the activation of caspase 3. This result is further confirmed by Western-blot analysis of abrin-treated cell lysate with anticaspase 3 antibody, which shows the appearance of a cleaved form of caspase 3 (Figure 3B).

Some closely related toxins like diptheria toxin [33] and Shiga toxin [34] have been reported to induce apoptosis by activating caspase 8, independent of the death receptor pathway, which prompted us to look at the involvement of caspase 8 in abrin-induced cell death. When Jurkat A3 I9.2 cells lacking expression of caspase 8 were treated with abrin, it was observed that there was no decrease in the apoptotic response (Figure 4A). Treatment of these cells with FasL, known to induce apoptosis in activated T-cells via caspase 8-mediated pathway, however, had no effect on these cells. Thus it can be inferred that abrin-induced cell-death pathway is independent of caspase 8 activation.

MMP perturbation by abrin

Measurement of $\triangle\Psi_m$ using the potentiometric dye, JC-1, revealed a marked decrease in $\triangle\Psi_m$ after a hyperpolarization phase. This hyperpolarization phase is seen up to 3 h of abrin treatment, after which $\triangle\Psi_m$ starts decreasing and reaches a minimum by 12 h (Figure 4B). This process is inhibited upon overexpression of Bcl-2 (Figure 5C). Thus it can be concluded that abrin induces stress-mediated apoptosis that follows the mitochondrial pathway.

Abrin induces ROS production

The fluorescent dye DCFH-DA was used to determine if the loss of $\triangle\Psi_m$ was due to ROS production in response to abrin. DCFH-DA is a non-fluorescent dye that gets converted into the active form by the action of intracellular esterases. This dye is then oxidized by oxygen radicals to its fluorescent form, which can be measured at 530 nm. In JR4 Jurkat cells, a time-dependent increase in fluorescence was observed upon treatment with 0.16 nM abrin and, by 12 h, a 35-fold increase in ROS production was observed as compared with untreated control (Figure 5D).

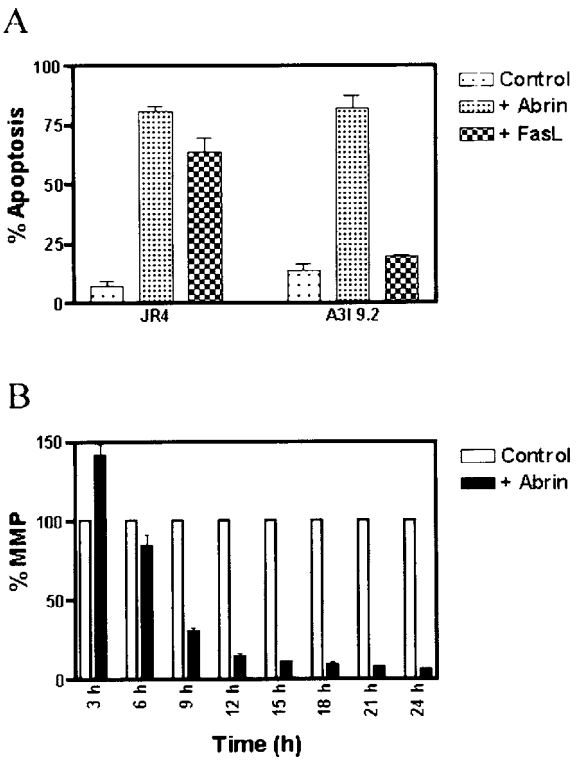

Figure 4 Abrin-induced apoptosis through intrinsic mitochondrial pathway

(**A**) Abrin-induced apoptosis is independent of caspase 8: A3 I9.2 Jurkat cells were treated in the presence or absence of abrin (0.16 nM) for 12 h and processed for FACS analysis after PI staining as mentioned earlier. FasL (10 ng/ml) was used as positive control. (**B**) Perturbation of $\triangle\Psi_m$ by abrin: after treatment with abrin or with PBS, Jurkat cells were stained with 2.5 μg/ml of JC-1 dye for 20 min at 37 °C, washed once with PBS containing 2 % FBS and analysed by flow cytometry. The percentage of cells having low $\triangle\Psi_m$ was calculated by taking the ratio of mean fluorescence intensities of the red to green fluorescence and were plotted against time.

Bcl-2 blocks abrin-induced apoptosis

Bcl-2 is an anti-apoptotic protein that is known to block the mitochondrial pathway of apoptosis. When the J16 Bcl-2 clone of Jurkat cells, which overexpresses Bcl-2, was treated with abrin, a marked decrease in apoptosis was observed, as measured by flow cytometry for DNA fragmentation (Figure 5B). However, no difference with respect to protein synthesis inhibition was seen when compared with JR4 Jurkat cells (Figure 5A). Also, the loss of $\triangle\Psi_m$ as well as ROS production were not observed in these cells (Figures 5C and 5D). This rescue of cells from abrin-induced apoptosis was not just due to a delay in the process, as cells were viable up to 72 h (results not shown). These experiments further confirmed that abrin-induced apoptosis follows the intrinsic mitochondrial pathway of apoptosis, and overexpression of Bcl-2 is enough to rescue cells from undergoing death.

DISCUSSION

Inhibitors of protein synthesis are known for their ability to induce apoptosis in cells, but the chronology of the events therein and the mechanism of apoptosis induction have not been delineated. This is of importance, because such a study may shed some light on the homeostasis mechanisms operating in cells and might also help

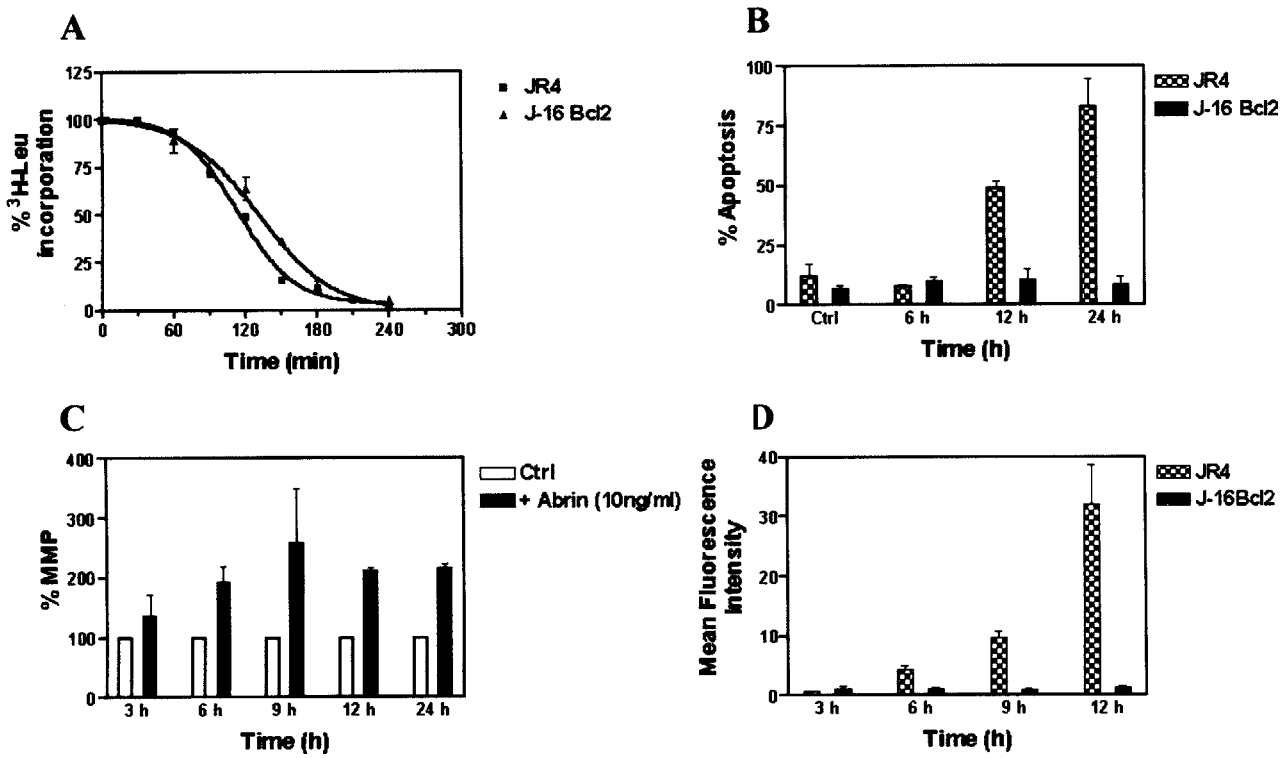

Figure 5 Abrin-induced apoptosis is blocked by Bcl-2 overexpression

(**A**) Abrin induces protein synthesis inhibition in J16 Bcl-2 cells: J16 Bcl-2 cells were treated with abrin for various time periods and processed as described earlier for [^{3}H]leucine incorporation. (**B**) J16 Bcl-2 cells are resistant to abrin-induced apoptosis: JR4 and J16 Bcl-2 Jurkat cells were cultured in the presence or absence of abrin and were processed as mentioned earlier and the DNA fragmentation was measured by PI staining and flow cytometry analysis. (**C**) Bcl-2 overexpression blocks abrin-induced $\triangle\Psi_m$ loss: J16 Bcl-2 cells cultured with or without abrin were stained with JC-1 as mentioned earlier and were analysed for $\triangle\Psi_m$. (**D**) Abrin-induced loss of $\triangle\Psi_m$ leads to ROS production: JR4 and J16 Bcl-2 Jurkat cells were preincubated with the dye DCFH-DA (20 μM) for 30 min at 37 °C followed by treatment with abrin. The cells were washed once and were analysed by flow cytometry for green fluorescence at 530 nm. The fold increase in mean fluorescence intensity over untreated control was plotted against time.

in elucidating the molecular switch that is involved in the induction of apoptosis due to protein synthesis inhibition. We have chosen the plant toxin, abrin, as the model protein synthesis inhibitor for such a study.

The toxicity of abrin is primarily due to inhibition of protein synthesis. The kinetics of protein synthesis inhibition shows that with increasing concentrations of abrin there is a decrease in the lag phase of protein synthesis inhibition, and a concentration of abrin as low as 0.16 nM showed complete inhibition of protein synthesis by 4 h, whereas apoptosis studies showed DNA fragmentation and cell death by 12 h. The kinetics of loss of $\triangle\Psi_m$, as measured by JC-1 staining, shows that this is the first apoptotic event triggered upon abrin treatment. JC-1 is a carbocyanine dye that stains mitochondria in viable cells when used at low concentrations. This cationic dye accumulates on the hyperpolarized mitochondrial inner membrane and leads to the formation of J aggregates that causes a shift in the emitted light from 530 nm (for the monomeric form of JC-1) to 590 nm (for the aggregate form). It was observed from the JC-1 staining (Figure 4B) that there is a loss of $\triangle\Psi_m$ after 6 h of abrin treatment. This suggests the possibility that abrin-induced apoptosis could occur by the mitochondrial pathway. Increase in ROS production was also detected at 6 h (Figure 5D), which could be the cause for or effect of loss in MMP (discussed below).

The next event to occur in inducing apoptosis is caspase 3 activation (Figures 3A and 3B). It is well documented that loss of $\triangle\Psi_m$ due to a permeability transition pore formation on mitochondrial membrane results in the release of cytochrome *c* into the cytosol, which in turn forms the apoptosome complex with apoptosis protease activating factor-1 and caspase 9 [35,36]. Activation of caspase 9 results in the activation of caspase 3 [37], which eventually leads to DNA fragmentation [32]. As observed by PI staining as well as agarose gel electrophoresis, there is a marked increase in DNA fragmentation 12 h after abrin treatment (Figures 2C and 3C). The involvement of other caspases has also been studied. Abrin treatment of A3 I9.2 Jurkat cells that lack caspase 8 revealed that there was no change in the magnitude of cell death by apoptosis (Figure 4A) when compared with JR4 cells (Figure 2C). This clearly showed that abrin-induced apoptosis does not follow a caspase 8-mediated pathway. Thus treatment of T-cells with abrin causes complete inhibiton of protein synthesis by 4 h. Apoptotic events start by 6 h with the loss of $\triangle\Psi_m$ and production of ROS. This is followed by caspase 3 activation, which leads to DNA fragmentation.

To understand the mitochondrial events better, a Jurkat clone overexpressing the anti-apoptotic protein Bcl-2 (J16 Bcl-2) was employed. Bcl-2 overexpression in these cells could rescue the cells from abrin-induced apoptosis (Figure 5B), but the kinetics of protein synthesis inhibition is identical with that of JR4 cells (Figure 5A). It is reported that Bcl-2 blocks MMP damage [38] and our studies confirmed it (Figure 5C). Also, the ROS production as measured by DCFH-DA fluorescence was decreased in these cells (Figure 5D). These observations suggest that ROS production by abrin is an effect of MMP damage, which leads to further apoptotic events. Therefore, mitochondria act as a control point in abrin-induced apoptosis.

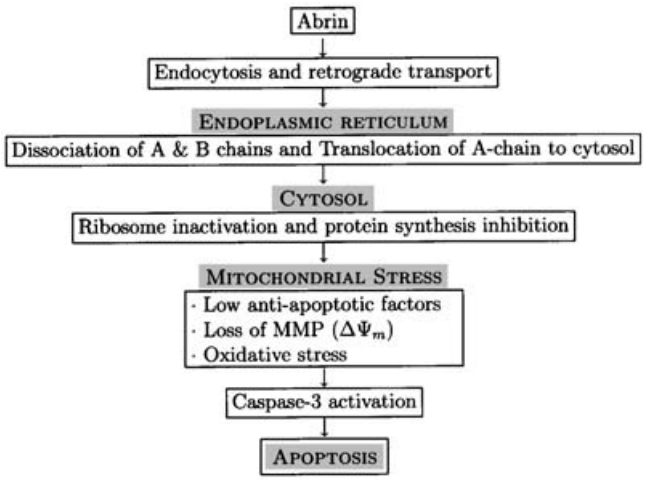

Figure 6 Schematic representation of the apoptotic pathway induced by abrin

Possible signals and pathways that could be involved in apoptosis induced by abrin are shown.

PARP [poly(ADP-ribose) polymerase] has been shown to induce the mitochondrial pathway of apoptosis, on hyperactivation in certain stress conditions due to depletion of the intracellular NAD^+ pool [39]. It has also been shown that ricin is capable of inducing depletion of intracellular NAD^+ and ATP levels, following PARP activation in U937 cells [17]. We examined the possibility of PARP involvement in abrin-induced mitochondrial damage. Studies using the PARP inhibitor 3-aminobenzamide did not show any rescue of abrin-induced apoptosis (results not shown) and hence NAD^+ depletion due to PARP hyper-activation, resulting in apoptosis is ruled out.

These studies raise the question as to why the inhibition of protein synthesis by an RIP should induce programmed cell death. Perhaps, an RIP inhibits the translation of a constitutive protein, which is continuously required to maintain the mitochondrial permeability transition pore in a closed state, keeping the apoptotic machinery in check. It has been reported that RNA and protein synthesis inhibitors, actinomycin D and cycloheximide respectively, can induce cell death in HL-60 cells [40,41]. Also, ML, another member of the type II family of RIPs, has been shown to induce apoptosis in the human T-lymphocyte cell line, MOLT-4. When Glu-166 and Arg-169 in the A-chain of ML were mutated to glutamine, the protein synthesis inhibitory as well as apoptosis-inducing capacity were reduced drastically [42]. Therefore, inhibition of protein synthesis is a requirement for apoptosis induction by RIPs.

In addition to plants, mammalian tissues have also been recently shown to harbour proteins that bring about adenine glycosylase activity under certain specific conditions. This activity is very similar to that of many plant RIPs and has been observed in extracts of cells or tissues under stress or infection [43]. We, therefore, propose the existence of a mechanism of cell-death induction that is triggered during cellular stress response similar to inhibition of protein synthesis. It is quite possible that the RIP toxins exploit this machinery to induce cell death.

In light of all these evidences, we propose that the apoptosis-inducing activity of abrin could be due to a decrease in levels of anti-apoptotic factors like Bcl-2 [44] and oxidative stress due to mitochondrial damage leading to increased ROS production (Figure 6).

We gratefully acknowledge Professor S. K. Podder for helpful scientific discussions. We thank Professor Schulze-Osthoff (Institute of Molecular Medicine, University of Duesseldorf, Germany) for his gift of J16 Bcl-2 clone of Jurkat cells. This work has been supported by grants from the Department of Science and Technology, the Department of Biotechnology and the Council of Scientific and Industrial Research, Government of India to A. S. and A. A. K. The help provided by Dr Omana Joy for the flow cytometry studies is also acknowledged.

REFERENCES

1 Tahirov, T. H., Lu, T. H., Liaw, Y. C., Chen, Y. L. and Lin, J. Y. (1995) Crystal structure of abrin-a at 2.14 Å. J. Mol. Biol. **250**, 354–367
2 Barbieri, L., Battelli, M. G. and Stirpe, F. (1993) Ribosome-inactivating proteins from plants. Biochim. Biophys. Acta **1154**, 237–282
3 Peumans, W. J., Hao, Q. and Van-Damme, E. J. (2001) Ribosome inactivating proteins from plants: more than RNA N-glycosidases. FASEB J. **15**, 1493–1506
4 Barbieri, L., Valbonesi, P., Bonora, E., Gorini, P., Bolognesi, A. and Stirpe, F. (1997) Polynucleotide: adenosine glycosidase activity of ribosome-inactivating proteins: effect on DNA, RNA and poly(A). Nucleic Acids Res. **25**, 518–522
5 Endo, Y. and Tsurugi, K. (1987) RNA N-glycosidase activity of ricin A-chain. Mechanism of action of the toxic lectin ricin on eukaryotic ribosomes. J. Biol. Chem. **262**, 8128–8130
6 Barbieri, L., Ferreras, J. M., Barraco, A., Ricci, P. and Stirpe, F. (1992) Some ribosome inactivating proteins depurinate ribosomal RNA at multiple sites. Biochem. J. **286**, 1–4
7 Sandvig, K. and van-Deurs, B. (2000) Entry of ricin and Shiga toxin into cells: molecular mechanisms and medical perspectives. EMBO J. **19**, 5943–5950
8 Lord, J. M. and Roberts, L. M. (1998) Toxin entry: retrograde transport through the secretory pathway. J. Cell Biol. **140**, 733–736
9 Barbieri, L., Battelli, M. G. and Stirpe, F. (1982) Reduction of ricin and other plant toxins by thiol:protein disulfide oxidoreductases. Arch. Biochem. Biophys. **216**, 380–383
10 Deeks, E. D., Cook, J. P., Day, P. J., Smith, D. C., Roberts, L. M. and Lord, J. M. (2002) The low lysine content of ricin a chain reduces the risk of proteolytic degradation after translocation from the endoplasmic reticulum to the cytosol. Biochemistry **41**, 3405–3413
11 Simpson, J. C., Roberts, L. M., Romisch, K., Davey, J., Wolf, D. H. and Lord, J. M. (1999) Ricin A chain utilises the endoplasmic reticulum-associated protein degradation pathway to enter the cytosol of yeast. FEBS Lett. **459**, 80–84
12 Bergamaschi, G., Perfetti, V., Tonon, L., Novella, A., Lucotti, C., Danova, M., Glennie, M. J., Merlini, G. and Cazzola, M. (1996) Saporin, a ribosome-inactivating protein used to prepare immunotoxins, induces cell death via apoptosis. Br. J. Haematol. **93**, 789–794
13 Bolognesi, A., Tazzari, P. L., Olivieri, F., Polito, L., Falini, B. and Stirpe, F. (1996) Induction of apoptosis by ribosome-inactivating proteins and related immunotoxins. Int. J. Cancer **68**, 349–355
14 Griffiths, G. D., Leek, M. D. and Gee, D. J. (1987) The toxic plant proteins ricin and abrin induce apoptotic changes in mammalian lymphoid tissues and intestine. J. Pathol. **151**, 221–229
15 Vervecken, W., Kleff, S., Pfuller, U. and Bussing, A. (2000) Induction of apoptosis by mistletoe lectin I and its subunits. No evidence for cytotoxic effects caused by isolated A- and B-chains. Int. J. Biochem. Cell Biol. **32**, 317–326
16 Komatsu, N., Oda, T. and Muramatsu, T. (1998) Involvement of both caspase-like proteases and serine proteases in apoptotic cell death induced by ricin, modeccin, diphtheria toxin, and pseudomonas toxin. J. Biochem. (Tokyo) **124**, 1038–1044
17 Komatsu, N., Nakagawa, M., Oda, T. and Muramatsu, T. (2000) Depletion of intracellular NAD^+ and ATP levels during ricin-induced apoptosis through the specific ribosomal inactivation results in the cytolysis of U937 cells. J. Biochem. (Tokyo) **128**, 463–470
18 Shih, S. F., Wu, Y. H., Hung, C. H., Yang, H. Y. and Lin, J. Y. (2001) Abrin triggers cell death by inactivating a thiol-specific antioxidant protein. J. Biol. Chem. **276**, 21870–21877
19 Hegde, R., Maiti, T. K. and Podder, S. K. (1991) Purification and characterization of three toxins and two agglutinins from *Abrus precatorius* seed by using lactamyl-Sepharose affinity chromatography. Anal. Biochem. **194**, 101–109
20 Matsumoto, I., Mizuno, Y. and Seno, N. (1979) Activation of Sepharose with epichlorohydrin and subsequent immobilization of ligand for affinity adsorbent. J. Biochem. (Tokyo) **85**, 1091–1098
21 Matsumoto, I., Seno, N., Golovtchenko-Matsumoto, A. M. and Osawa, T. (1980) Amination and subsequent derivatization of epoxy-activated agarose for the preparation of new affinity adsorbents. J. Biochem. (Tokyo) **87**, 535–540
22 Sharma, S., Podder, S. K. and Karande, A. A. (1999) Comparative studies on kinetics of inhibition of protein synthesis in intact cells by ricin and a conjugate of ricin B-chain with momordin. Mol. Cell. Biochem. **200**, 133–141

23 McGahon, A. J., Martin, S. J., Bissonnette, R. P., Mahboubi, A., Shi, Y., Mogil, R. J., Nishioka, W. K. and Green, D. R. (1995) The end of the (cell) line: methods for the study of apoptosis *in vitro*. Methods Cell Biol. **46**, 172–173
24 Fraker, P. J., King, L. E., Lill-Elghanian, D. and Telford, W. G. (1995) Quantification of apoptotic events in pure and heterogenous populations of cells using flow cytometer. Methods Cell Biol. **46**, 60–61
25 Gong, J., Traganos, F. and Darzynkiewicz, Z. (1994) A selective procedure for DNA extraction from apoptotic cells applicable for gel electrophoresis and flow cytometry. Anal. Biochem. **218**, 314–319
26 Cossarizza, A., Baccarani-Contri, M., Kalashnikova, G. and Franceschi, C. (1993) A new method for the cytofluorimetric analysis of mitochondrial membrane potential using the J-aggregate forming lipophilic cation 5,5′,6,6′-tetrachloro-1,1′,3,3′-tetraethyl-benzimidazolcarbocyanineiodide (JC-1). Biochem. Biophys. Res. Commun. **197**, 40–45
27 Bass, D. A., Parce, J. W., Dechatelet, L. R., Szejda, P., Seeds, M. C. and Thomas, M. (1983) Flow cytometric studies of oxidative product formation by neutrophils: a graded response to membrane stimulation. J. Immunol. **130**, 1910–1917
28 Hegde, R. and Podder, S. K. (1997) A- and B-subunit variant distribution in the holoprotein variants of protein toxin abrin: variants of abrins I and III have constant toxic A subunits and variant lectin B subunits. Arch. Biochem. Biophys. **344**, 75–84
29 Hegde, R., Karande, A. A. and Podder, S. K. (1993) The variants of the protein toxins abrin and ricin. A useful guide to understanding the processing events in the toxin transport. Eur. J. Biochem. **215**, 411–419
30 Thornberry, N. A. and Lazebnik, Y. (1998) Caspases: enemies within. Science **281**, 1312–1316
31 Stennicke, H. R. and Salvesen, G. S. (1997) Biochemical characteristics of caspases-3, -6, -7, and -8. J. Biol. Chem. **272**, 25719–25723
32 Enari, M., Sakahira, H., Yokoyama, H., Okawa, K., Iwamatsu, A. and Nagata, S. (1998) A caspase-activated DNase that degrades DNA during apoptosis, and its inhibitor ICAD. Nature (London) **391**, 43–50
33 Thorburn, J., Frankel, A. E. and Thorburn, A. (2002) Apoptosis by leukemia cell-targeted diphtheria toxin occurs via receptor-independent activation of Fas-associated death domain protein. Clin. Cancer Res. **9**, 861–865
34 Ching, J. C., Jones, N. L., Ceponis, P. J., Karmali, M. A. and Sherman, P. M. (2002) *Escherichia coli* Shiga-like toxins induce apoptosis and cleavage of poly(ADP-ribose) polymerase via *in vitro* activation of caspases. Infect. Immunol. **70**, 4669–4677
35 Li, P., Nijhawan, D., Budihardjo, I., Srinivasula, S. M., Ahmad, M., Alnemri, E. S. and Wang, X. (1997) Cytochrome *c* and dATP-dependent formation of Apaf-1/caspase-9 complex initiates an apoptotic protease cascade. Cell (Cambridge, Mass.) **91**, 479–489
36 Petronilli, V., Penzo, D., Scorrano, L., Bernardi, P. and Di-Lisa, F. (2001) The mitochondrial permeability transition, release of cytochrome *c* and cell death. Correlation with the duration of pore openings *in situ*. J. Biol. Chem. **276**, 12030–12034
37 Kuida, K., Haydar, T. F., Kuan, C. Y., Gu, Y., Taya, C., Karasuyama, H., Su, M. S., Rakic, P. and Flavell, R. A. (1998) Reduced apoptosis and cytochrome *c*-mediated caspase activation in mice lacking caspase 9. Cell (Cambridge, Mass.) **94**, 325–337
38 Susin, S. A., Zamzami, N., Castedo, M., Hirsch, T., Marchetti, P., Macho, A., Daugas, E., Geuskens, M. and Kroemer, G. (1996) Bcl-2 inhibits the mitochondrial release of an apoptogenic protease. J. Exp. Med. **184**, 1331–1341
39 Ha, H. C. and Snyder, S. H. (2000) Poly(ADP-ribose) polymerase-1 in the nervous system. Neurobiol. Dis. **7**, 225–239
40 Martin, S. J., Lennon, S. V., Bonham, A. M. and Cotter, T. G. (1990) Induction of apoptosis (programmed cell death) in human leukemic HL-60 cells by inhibition of RNA or protein synthesis. J. Immunol. **145**, 1859–1867
41 Martin, S. J. (1993) Protein or RNA synthesis inhibition induces apoptosis of mature human $CD4^+$ T cell blasts. Immunol. Lett. **35**, 125–134
42 Langer, M., Mockel, B., Eck, J., Zinke, H. and Lentzen, H. (1999) Site-specific mutagenesis of mistletoe lectin: the role of RIP activity in apoptosis. Biochem. Biophys. Res. Commun. **264**, 944–948
43 Barbieri, L., Valbonesi, P., Bondioli, M., Alvarez, M. L., Dal-Monte, P., Landini, M. P. and Stirpe, F. (2001) Adenine glycosylase activity in mammalian tissues: an equivalent of ribosome-inactivating proteins. FEBS Lett. **505**, 196–197
44 Hu, R., Zhai, Q., Liu, W. and Liu, X. (2001) An insight into the mechanism of cytotoxicity of ricin to hepatoma cell: roles of Bcl-2 family proteins, caspases, Ca^{2+}-dependent proteases and protein kinase C. J. Cell. Biochem. **81**, 583–593

Received 30 May 2003/12 August 2003; accepted 16 September 2003
Published as BJ Immediate Publication 16 September 2003, DOI 10.1042/BJ20030797